Title

Materials Genomics Screens for Adaptive Ion Transport Behavior by Redox-Switchable Microporous Polymer Membranes in Lithium–Sulfur Batteries

Journal

ACS Central Science, 3(5)

ISSN

2374-7943

Authors

Ward, Ashleigh L

Doris, Sean E

Li, Longjun

et al.

Publication Date

2017-05-24

DOI

10.1021/acscentsci.7b00012

Peer reviewed

ACS central science

Research Article

http://pubs.acs.org/journal/acscii

Materials Genomics Screens for Adaptive Ion Transport Behavior by Redox-Switchable Microporous Polymer Membranes in Lithium–Sulfur Batteries

Ashleigh L. Ward,[†] Sean E. Doris,[‡] Longjun Li,[†] Mark A. Hughes, Jr.,[§] Xiaohui Qu,[†,∥] Kristin A. Persson,[†,∥,⊥] and Brett A. Helms*[,†,#]

[†]The Joint Center for Energy Storage Research, [∥]Computational Research Division, and [#]The Molecular Foundry, Lawrence Berkeley National Laboratory, 1 Cyclotron Road, Berkeley, California 94720, United States

[‡]Department of Chemistry, [§]Department of Chemical and Biomolecular Engineering, and [⊥]Department of Materials Science and Engineering, University of California, Berkeley, California 94720, United States

Supporting Information

ABSTRACT: Selective ion transport across membranes is critical to the performance of many electrochemical energy storage devices. While design strategies enabling ion-selective transport are well-established, enhancements in membrane selectivity are made at the expense of ionic conductivity. To design membranes with both high selectivity and high ionic conductivity, there are cues to follow from biological systems, where regulated transport of ions across membranes is achieved by transmembrane proteins. The transport functions of these proteins are sensitive to their environment: physical or chemical perturbations to that environment are met with an adaptive response. Here we advance an analogous strategy for achieving adaptive ion transport in microporous polymer membranes. Along the polymer backbone are placed redox-active switches that are activated in situ, at a prescribed electrochemical potential, by the device's active materials when they enter the membrane's pore. This transformation has little influence on the membrane's ionic conductivity; however, the active-material blocking ability of the membrane is enhanced. We show that when used in lithium–sulfur batteries, these membranes offer markedly improved capacity, efficiency, and cycle-life by sequestering polysulfides in the cathode. The origins and implications of this behavior are explored in detail and point to new opportunities for responsive membranes in battery technology development.

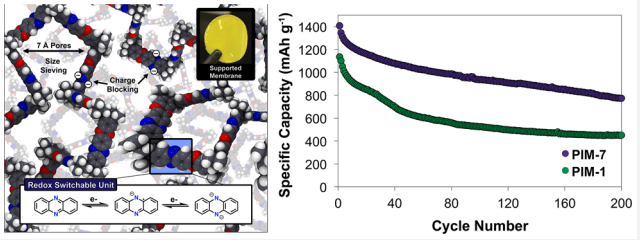

INTRODUCTION

Membranes play a critical role in many battery technologies, where they serve to electronically isolate the anode from the cathode and allow the battery's working ion to diffuse between them.[1,2] For battery chemistries that involve active materials that are dissolved, dispersed, or suspended in electrolyte, membranes must also prevent active-material crossover; failure to do so leads to low round-trip energy efficiency and in some cases unacceptable capacity fade.[3−5] This is particularly problematic in lithium–sulfur (Li–S) batteries, where inefficiencies and instabilities arise when soluble polysulfides—intermediates in the electrochemical interconversion of S_8 and Li_2S—cross over and incur a shuttling current or irreversibly react with the lithium–metal anode.[6−12] While a number of strategies have been suggested for solving the polysulfide shuttle, including the use of lithiated Nafion[13] membranes and polymer,[14] carbon,[15,16] or ceramic-coated separators,[14,15] none of these approaches were capable of complete blocking of polysulfide crossing without incurring dramatic losses in ionic conductivity.

Here we show that these shortcomings are alleviated in the Li–S battery when its membrane is rationally configured from new redox-switchable polymers of intrinsic microporosity (PIMs) (Figure 1).[17−21] Key to our success is the adaptation of the membrane's transport selectivity for the battery's working ion in situ. More specifically, we leverage the reducing environment of the sulfur cathode to chemically transform a charge-neutral and size-selective PIM membrane into a lithiated and anionic PIM membrane with enhanced polysulfide-rejecting properties. Our in situ activation strategy sidesteps well-known polymer processing challenges encountered with ionomers, where ion clustering into nonpercolating microphase-separated domains is prevalent and renders the material resistive to ion transport.[22−25]

The design of adaptive PIM membranes was computationally guided using a materials genome,[26−28] where candidate monomer segments were screened for their susceptibility to reduction by polysulfides (i.e., a reduction potential above 2.5 V vs Li/Li^+). We experimentally validated these predictions and were further able to demonstrate that progressive reduction and lithiation of the PIM membrane by polysulfides slows

Received: January 6, 2017
Published: April 27, 2017

DOI: 10.1021/acscentsci.7b00012
ACS Cent. Sci. 2017, 3, 399−406

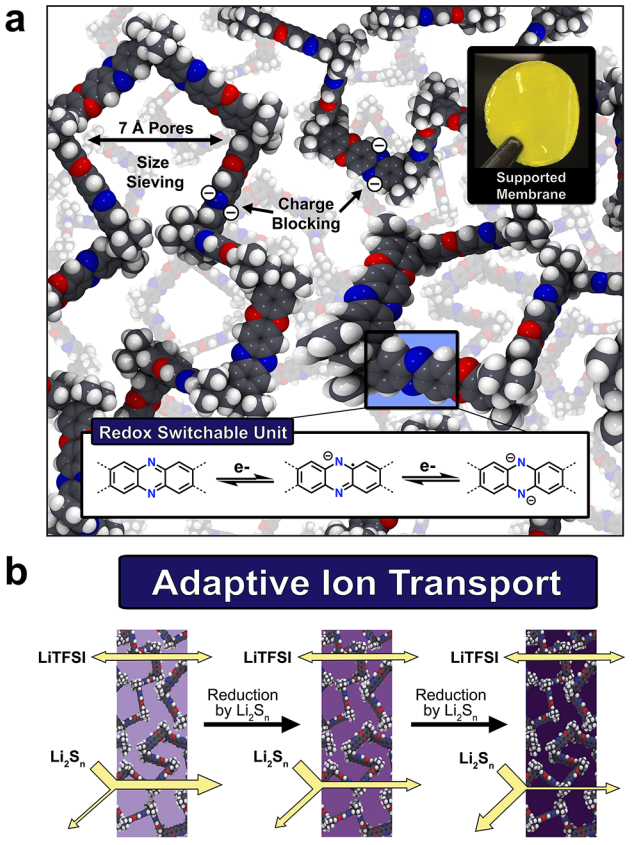

Figure 1. Directed evolution of a microporous polymer membrane's ion-transport selectivity. (a) The ion-transport selectivity of membranes cast from polymers of intrinsic microporosity (PIMs) (top right inset) can be enhanced to the benefit of Li−S battery cycle-life when redox-switchable phenazine-containing monomers are activated in situ (bottom left inset) by endogenous reducing polysulfides (Li_2S_n, for n = 4−8). (b) This leads to a feedback loop whereby progressive reduction of the membrane by adventitious polysulfides only serves to further restrict their access to the membrane's pore voids.

polysulfide diffusive permeability from 1.7×10^{-10} to 9.2×10^{-11} cm^2 s^{-1}—an impressive 570-fold improvement over nonselective Celgard separators[1]—without significantly impacting the membrane's ionic conductivity ($\sigma = 5 \times 10^{-3}$ mS cm^{-1} at 298 K). We also showed that by blocking polysulfide crossover, the Coulombic efficiency and cycle-life of Li−S cells greatly improves—most notably in the absence of lithium-anode protecting additives.[29−32] The stability of the lithium metal anode under these conditions is unprecedented and highlights the unexpected and exciting new opportunities afforded by responsive redox-active polymers, and ultimately adaptive membranes, in battery technology development.

RESULTS AND DISCUSSION

PIMs are a compelling and versatile platform to understand structure-transport relationships in microporous polymer membranes. Transport outcomes are rationalized on the basis of membrane porosity and pore architecture and their relation to the species interacting with the membrane.[17−21,33] The membrane's structural characteristics are dictated by polymer chain-packing relationships,[34−36] and these packing relationships are ultimately determined by monomer segments within polymer chains,[19−21] polymer processing techniques used to cast the membrane,[37−39] and membrane−electrolyte interactions.[40] In the past, PIMs have advanced as membranes with passive, nontransformable architectures; these membranes are overwhelmingly used for selective gas transport.[17−21] In the context of a Li−S battery, however, a myriad of chemical transformations can take place.[41−46] Therefore, we reasoned that PIM membranes need not be inactive; instead, they might serve as adaptive components whose microporous architectures are switchable, dynamic, and tailored at the molecular level to respond to local chemical cues within the battery's electrolyte—in this case lithium polysulfides (Li_2S_n, for n = 4−8), which are endogeneous to Li−S batteries. The ability of these new PIM membranes to adapt and sustain their polysulfide-blocking ability in situ is unusual and offers advantages over traditional approaches based on single-ion conducting membranes[13,47,48] and other permselective barriers[49−52] whose beneficial properties are ultimately transient. The origin of this transience is tied to the use of anode-protecting additives in the electrolyte (e.g., $LiNO_3$), which are consumed until exhausted and their stabilizing effects are lost thereafter.[29−32]

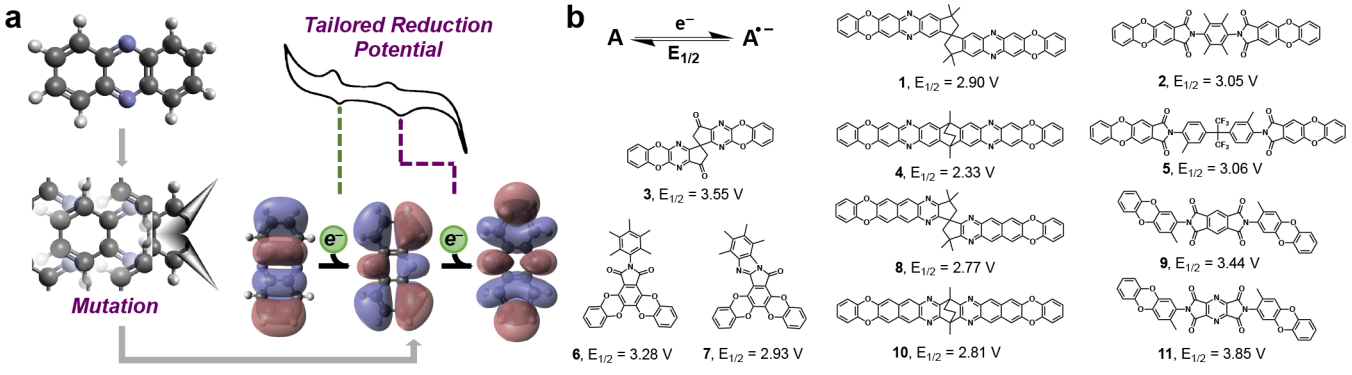

Figure 2. Predictive design of redox-switchable monomer segments for adaptive microporous polymer membranes tailored for lithium−sulfur batteries. (a) A library of redox-active compounds was generated and screened computationally using a materials genome, seeking to identify those with reduction potentials ($E_{1/2}$) higher than 2.5 V vs Li/Li$^+$; monomers passing this screen would indicate they are readily reduced by lithium polysulfides present in the battery electrolyte. (b) Atom-by-atom substitutions in various PIM-monomer segments led to a number of hits passing our fitness test for $E_{1/2}$. PIMs incorporating lead compound **1** are known as PIM-7. Battery membranes derived from PIM-7 are thus expected to provide access to a new type of membrane that adapts its ion-transporting behavior by engaging the battery's intrinsic chemistry for storing and releasing charge.

DOI: 10.1021/acscentsci.7b00012
ACS Cent. Sci. 2017, 3, 399−406

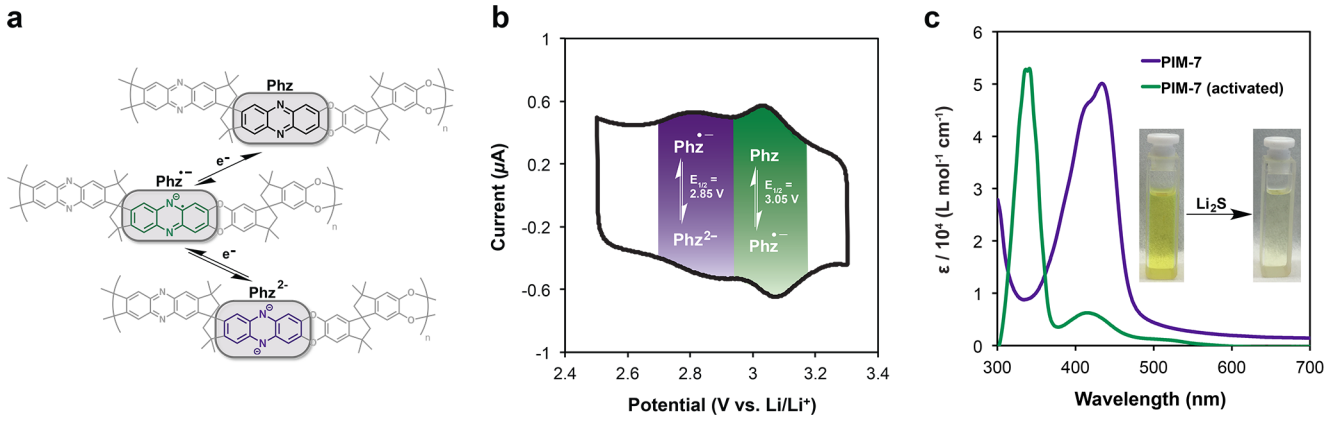

Figure 3. Direct evidence that PIM-7 is reduced to a dilithiated state in the desired potential window for a lithium−sulfur battery and that this reduction occurs on contact with sulfur-based reductants. (a) Molecular outcomes of the sequential chemical reduction of PIM-7. (b) Cyclic volammogram of PIM-7 on a glassy carbon working electrode. Two reversible reductions are observed at $E_{1/2}$ = 3.05 and 2.85 V vs Li/Li$^+$, consistent with a stepwise two-electron reduction of the polymer's phenazine units (inset). (c) UV−vis extinction spectra of PIM-7 before and after chemical reduction with Li_2S in THF.

Materials Genomics Screens for PIM Membranes with Adaptive Ion Transport Behaviors. To confer adaptive transport behaviors to PIM membranes, we implemented a materials genome to screen a library of candidate monomer segments for switchable redox properties (Figure 2)—and more specifically, for a reduction potential ($E_{1/2}$) higher than 2.5 V vs Li/Li$^+$. The library design focused on phenazines (e.g., **1** and **4**), 1*H*-isoindole-1,3(2*H*)-diones (e.g., **2**, **5**, and **6**), pyrazines (e.g., **3**), *H*-isoindolo[2,1-*a*]benzimidazol-11-ones (e.g., **7**), benzo[*g*]quinoxalines (e.g., **8** and **10**), benzo[1,2-*c*:4,5-*c*′]dipyrrole-1,3,5,7(2*H*,6*H*)-tetrones (e.g., **9**), and dipyrrolo[3,4-*b*:3′,4′-*e*]pyrazine-1,3,5,7(2*H*,6*H*)-tetrones (e.g., **11**)—all of which in principle could be reduced and lithiated at oxygen or at nitrogen centers upon interaction with Li_2S_n. For example, members of the library containing 1*H*-isoindole-1,3(2*H*)-dione substituents are predicted to be reduced by polysulfides to their lithiated radical anions, while others containing diazaheterocycles were designed to undergo sequential reductions to a closed-shell dianionic (and dilithiated) state, in some cases driven by rearomatization (e.g., **1** and **4**).

The molecular structure and reduction potential of the PIM membrane segments were predicted using density functional theory (DFT).[53,54] As lithium cations can bind to any of the electronegative heteroatoms in the monomer segments, the most favorable binding site was identified by comparing the DFT-predicted energy of all possible Li$^+$-O/N binding configurations. The reduction potential ($E_{1/2}$) was then predicted by calculating the adiabatic electronic affinity of the segments in the delithiated state.[26,27] Structure relaxation and energy evaluation were carried out using the M08-SO functional,[55] while solvent effects were captured by either the IEF-PCM or SMD implicit solvent models,[56] where the dielectric constant value was set to the experimentally determined value of 9.0 for the battery electrolyte (Figure S8). All DFT calculations were performed using the Q-Chem software package.[57]

Many candidates in the library passed our initial screen (Figure 2b). To discriminate between hits, we noted that PIMs based on **2**, **5**, **6**, and **9** typically form brittle films that preclude use as a flexible membrane. We further hypothesized that closed-shell dianionic outcomes may provide more chemical stability long-term, and thus our focus turned to monomers containing phenazines. Charge-neutral PIMs derived from phenazine-containing monomer segment **1** (calculated $E_{1/2}$ = 2.90 V for the first peak and 2.28 V for the second peak vs Li/Li$^+$) are known as PIM-7;[18,58] however, the redox-active character of these polymers has not been reported previously nor has their ion-transporting ability as a membrane.

Validation of Candidate PIM Membrane Redox Chemistry with Lithium Polysulfides. To validate our predictions, we first synthesized PIM-7 via step-growth polymerization in 78% yield and M_n of 80 kg mol^{-1}. Care was taken to adapt the synthetic methodology to afford PIM-7 with high molecular weight as needed to cast flexible membranes (see Supporting Information). With high molecular weight PIM-7 in hand, we then carried out cyclic voltammetry (CV) on the polymer drop-cast onto a glassy carbon working electrode. PIM-7 exhibited two reversible reduction peaks at $E_{1/2}$ = 3.05 and 2.85 V vs Li/Li$^+$, consistent with the reduction of the phenazine unit to the radical anion followed by the reduction to the dianionic species (Figure 3a). We noted that while the first reduction was within the range predicted by the genome screen, the second was not. We were able to resolve this incongruity in part by taking into account solvent effects using the SMD solvation model,[59] which addresses solute−solvent dispersion interactions that are lacking in the currently available IEF-PCM model. Specifically, the experimentally measured dielectric constant of the electrolyte used in this work was used to simulate the electrostatic interaction for both the IEF-PCM and SMD implicit solvent models. The CDS (cavitation/dispersion/solvent-structure) parameters for the SMD were chosen to simulate the effect of the diglyme solvent: the index of refraction, surface tension, and Abraham's hydrogen bond basicity were set to 1.4097, 36.83, and 0.859, respectively; all other CDS parameters (aromaticity, electronegative halogenicity, and Abraham's hydrogen bond acidity) were set to 0.0. Within the SMD context, we calculated $E_{1/2}$ = 3.31 V for the first peak and 2.75 V for the second peak (vs Li/Li$^+$) for **1**. The implication here is that understanding the second chemical reduction from a lithiated radical anion to a dilithiated dianionic species benefits from the SMD treatment and is likely to best apply to the molecules in the library with multiple redox processes. In parallel, we also demonstrated

DOI: 10.1021/acscentsci.7b00012
ACS Cent. Sci. 2017, 3, 399−406

experimentally that PIM-7 could be chemically reduced when introduced to a dilute solution of Li_2S. The optical signatures of PIM-7 in its charge neutral and dianionic state were readily distinguished by UV−Vis spectroscopy (Figure 3b), with wavelength-shifts in the extinction maxima of 440−330 nm consistent with increased electron density of the polymer in its reduced state. Taken together, these results confirmed that PIM-7 membranes will become negatively charged and lithiated in the reducing environment of the Li−S battery as predicted from the materials genomics screen.

Quantitative Understanding of the Adaptive Ion Transport Behavior of PIM-7 Membranes with Lithium Polysulfides Present. Ion-selective membranes were prepared by casting PIM-7 as a thin layer on a mesoporous Celgard 2325 support using a wire-wound rod coating process.[60] This method afforded uniform, 2 μm-thick coatings of PIM-7 on the flexible polymer support as evidenced by cross-sectional SEM (Figure S10). The packing of polymer chains for PIM-7 in the dry state yields an average pore size of 0.70 nm for the membrane (Figure S11).[18,59] This size regime is predicted to be ideal for sieving polysulfides by size in battery electrolyte.[40]

In order to confirm that PIM-7 selective layers block polysulfide crossover, we carried out crossover measurements using native supported PIM-7 membranes of a known area and thickness placed between two compartments of a diffusion cell (i.e., an H-cell). The H-cell was configured with dissolved Li_2S_n (0.8 M S as Li_2S_8 in diglyme containing 0.50 M LiTFSI and 0.15 M $LiNO_3$) on the retentate side and Li_2S_n-free electrolyte on the permeate side (Figure 4a, and the cell shown in the inset of Figure 4b). The diffusion of Li_2S_n to the permeate side was then monitored for up to 15 h using CV, where the concentration of polysulfides could be directly related to the measured peak current in the CV using a calibration curve determined separately for a 1−50 mM concentration regime for Li_2S_n (Figure S12). We carried out the same experiments on unmodified Celgard separators, which are known to be poorly selective for Li_2S_n (negative control), and for PIM-1 on Celgard, which has been reported by us[40] to provide selectivity but not adaptability (positive control). From these data, we were able calculate effective diffusive permeabilities ($D_{eff,membrane}$) of Li_2S_n through Celgard and PIM on Celgard layered hybrid membranes. After measuring $D_{eff,membrane}$ for Celgard alone, we were able to extract the effective diffusive permeability of Li_2S_n through the PIM selective layer, $D_{eff,selective}$, from $D_{eff,membrane}$ of Li_2S_n through the layered membranes (see Supporting Information). This analysis returned $D_{eff,selective}$ values of D_{eff} = (5.2 ± 0.4) × 10^{-8} cm^2 s^{-1} for Celgard; (4.3 ± 0.3) × 10^{-10} cm^2 s^{-1} for PIM-1 on Celgard; and (1.7 ± 0.1) × 10^{-10} cm^2 s^{-1} for PIM-7 on Celgard without any Li_2S_n pretreatment. Thus, PIM-7 represents the best size-selective membrane for blocking Li_2S_n crossover to date, with diffusive permeabilities for Li_2S_n that are 2.5- and 306-fold lower than PIM-1 and Celgard, respectively (Table 1).

We next sought to understand the impact of polysulfide-driven reductive chemical transformations on the polysulfide-blocking ability of PIM-7 membranes over time. To do so, PIM-7 membranes were bathed in concentrated solutions of Li_2S_n (1.0 M S as Li_2S_8 in diglyme containing 0.50 M LiTFSI and 0.15 M $LiNO_3$) for a prescribed period, either 12 or 24 h, and then rinsed with and soaked in fresh electrolyte. The crossover data showed that PIM-7's polysulfide-blocking ability is enhanced as the phenazine units are progressively reduced

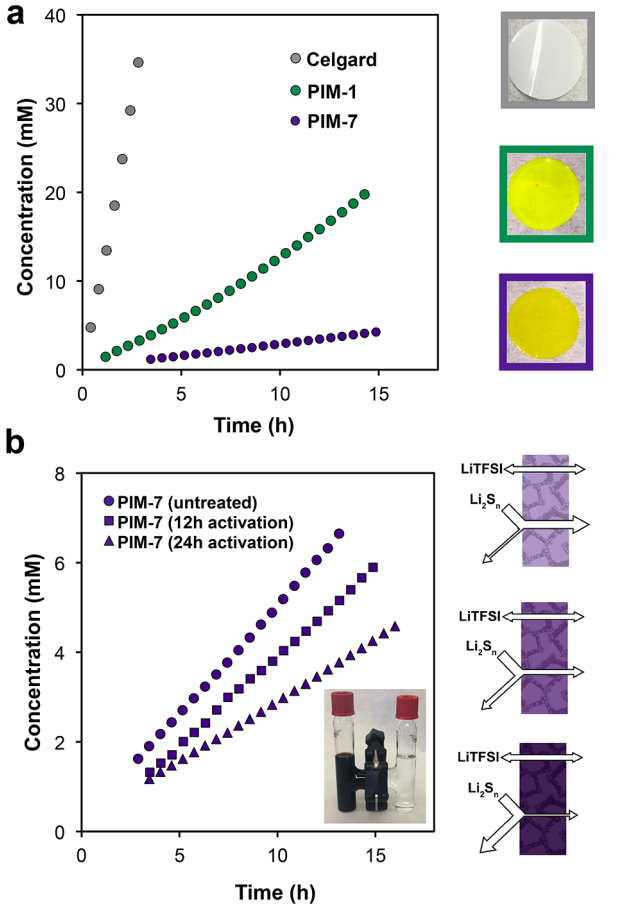

Figure 4. Superior polysulfide-blocking ability by supported PIM-7 membranes and their adaptive transport behaviors in response to Li_2S_n. Time evolution of Li_2S_n concentration in the permeate (right) of H-cells equipped with (a) Celgard (gray), supported PIM-1 (green) or supported PIM-7 (purple) membranes and (b) supported PIM-7 membranes prereduced for 0, 12, or 24 h. The retentate was charged with an initial concentration of 0.8 M S as Li_2S_8 in electrolyte. Data obtained at times <3 h were below the limit of quantification and were thus omitted.

Table 1. Performance Metrics Distinguishing Non-Selective, Selective, and Adaptive Polymer Membranes

membrane	membrane ionic conductivity (mS cm^{-1})	polysulfide diffusive permeability (cm^2 s^{-1})
Celgard 2325	1.36 × 10^{-1}	(5.2 ± 0.4) × 10^{-8}
PIM-1 on Celgard	5.9 × 10^{-3}	(4.3 ± 0.3) × 10^{-10}
native PIM-7 on Celgard (0 h)	(7 ± 2) × 10^{-3}	(1.7 ± 0.1) × 10^{-10}
activated PIM-7 on Celgard (24 h)	(5 ± 3) × 10^{-3}	(9.2 ± 0.7) × 10^{-11}

over time by Li_2S_n (Figure 4b). From these data, we were also able to quantify the evolutionary changes in Li_2S_n diffusive permeability from the baseline of (1.7 ± 0.1) × 10^{-10} cm^2 s^{-1} for PIM-7 on Celgard in its initial state, to (1.4 ± 0.1) × 10^{-10} cm^2 s^{-1} after 12 h and (9.2 ± 0.7) × 10^{-11} cm^2 s^{-1} after 24 h of chemical transformation. Extended application of Li_2S_n beyond 24 h did not appear to further enhance the membrane's polysulfide-blocking ability. We attribute this effect to the slow diffusion of polysulfides through the membrane and the feedback loop associated with the reduced form of the membrane further retarding the migration of additional

DOI: 10.1021/acscentsci.7b00012
ACS Cent. Sci. 2017, 3, 399−406

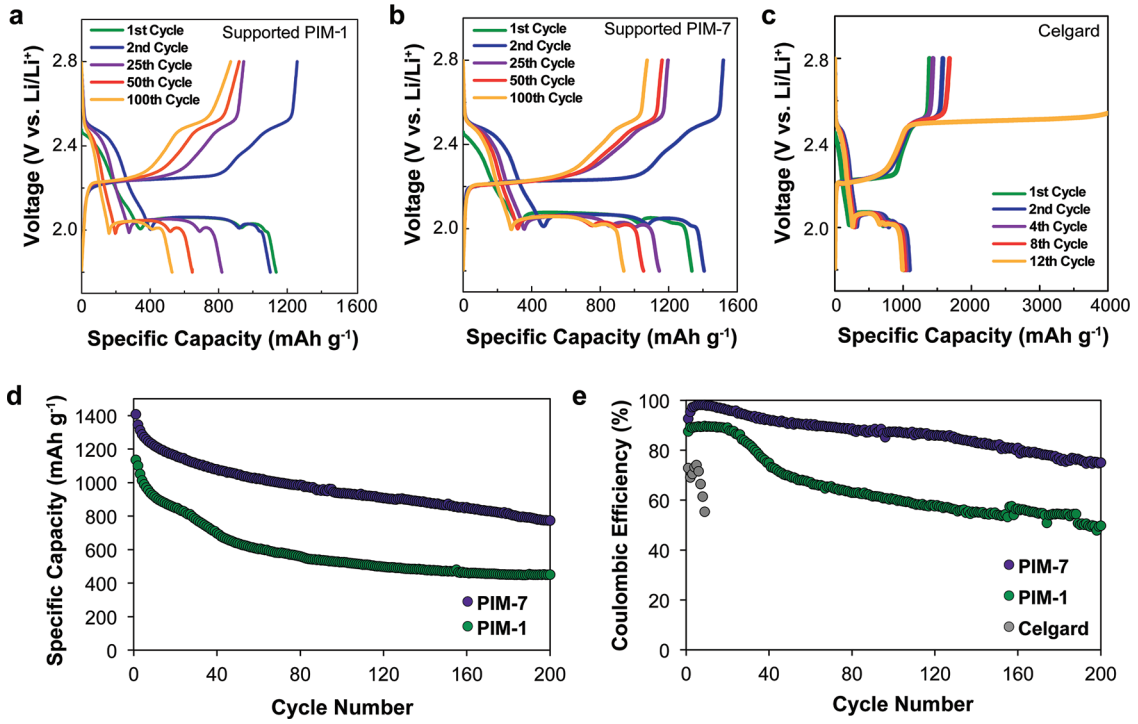

Figure 5. Putting the adaptive polysulfide-blocking ability of supported PIM-7 membranes to work in Li−S electrochemical cells. Discharge and charge capacity profiles for Li−S cells equipped with (a) PIM-1 on Celgard, (b) PIM-7 on Celgard, and (c) Celgard alone. (d) Long-term cycling data at a rate of C/8 for Li−S cells showing (d) improved capacity retention and (e) Coulombic efficiency for cells equipped with PIM-7 membranes. Li−S cells with superior performance could be prepared with prereduced and lithiated PIM-7 on Celgard or, alternatively, with native PIM-7 on Celgard. In the case of the latter, a membrane activation period of up to 24 h before initiating cycling was advantageous.

polysulfides. Thus, the membrane adapts its transport behavior and sustains these functions indefinitely; indeed, supported PIM-7 membranes demonstrated a stable crossover rate for at least 2 days. Advantageously, while the polysulfide-blocking character of supported PIM-7 membranes was enhanced upon increasing reduction of the phenazine subunits, the membrane ionic conductivity remained largely unchanged at 5×10^{-3} mS cm^{-1} (Table 1 and Figure S14).

Implementation of Adaptive PIM-7 Membranes in Lithium−Sulfur Cells. The superior polysulfide blocking ability of adaptive PIM-7 membranes over nonselective Celgard and passively selective PIM-1 membranes had a profound effect on the sulfur utilization, energy efficiency, and cycle-life of Li−S batteries (Figure 5a−c). Here we assembled Li−S coin cells using a dissolved polysulfide cathode, whereby a semisolid ink containing Li_2S_n (1.0 M S as Li_2S_8 in diglyme containing 0.50 M LiTFSI) and Ketjenblack (5% w/w) was introduced to a high surface-area carbon nanofiber current collector.[45,61−63] In this configuration, a high concentration of polysulfides is in direct contact with the membrane; this presents the most aggressive fitness test for the different membrane constructs. All coin cells were tested using electrolytes that were devoid of $LiNO_3$ as an anode- protecting additive; in doing so, the Coulombic inefficiencies associated with the polysulfide shuttle can only be improved upon by an ion-selective membrane. All cells were galvanostatically cycled between 1.8−2.8 V at a C/8 rate for up to 200 cycles.

Cells assembled with nonselective Celgard separators (negative control) were prone to Coulombic (and energy) inefficiencies associated with the polysulfide shuttle as has been previously reported.[6,29−32] As these cells were cycled, the charging cycle required additional energy with each cycle until the twelfth cycle, at which point the charging cycle continued indefinitely (Figure 5c). On the other hand, Li−S cells assembled with passively selective PIM-1 membranes on Celgard (positive control, Figure 5a) were significantly more effective at arresting the polysulfide shuttle; no infinite-charge regime was observed and the energy required to fully recharge these cells was sustainably low. The sulfur utilization of these cells (~1100 mA h g^{-1} after the second-cycle discharge) was on par with cells assembled with Celgard, as was the capacity fade in the first few cycles; however, the cycle-life of these cells was significantly extended to 200 cycles. The specific capacity of PIM-1 cells at the end of 200 cycles was 451 mA h g^{-1} with a capacity fade of 0.302% per cycle.

In contrast to cells assembled with either Celgard alone or PIM-1 on Celgard, those assembled with adaptive membranes consisting of PIM-7 on Celgard (Figure 5e) were most effective at preventing the polysulfide shuttle. The initial Coulombic efficiency of these cells was high (92.6%, compared to 87.5% for PIM-1 on Celgard and 72.9% for Celgard alone). We also noted that these cells gave markedly improved sulfur utilization, with a specific capacity of 1407 mA h g^{-1} (~20% enhancement over both Celgard and PIM-1 on Celgard, and 88% of theoretical); this is consistent with their chemically evolved ability to better sequester the polysulfides to the sulfur cathode. Furthermore, cells assembled with PIM-7 on Celgard were able to sustain capacities of 774 mA h g^{-1} (55% of initial) over 200 cycles, with a capacity fade of 0.225% per cycle. This result is highly unusual given that there are no anode-protecting $LiNO_3$ additives present in the electrolyte, highlighting the important role played by the redox-switchable character of the PIM-7 membrane in enabling and sustaining excellent Li−S cell performance. Notably, the versatile yet powerful aspects noted

DOI: 10.1021/acscentsci.7b00012
ACS Cent. Sci. 2017, 3, 399−406

here for an adaptive membrane design are completely overlooked in conventional polymeric and composite ion-transporting materials used in Li−S cells. It is likely that such membranes will find synergistic use in Li−S cells with other advances in sulfur cathodes,[64] electrolytes,[65] and lithium−metal protection schemes.[66,67]

CONCLUSIONS

The emerging view from our work is that macromolecular design strategies for ion-selective polymer membranes are primed for a paradigm-shift. It is now possible to use the redox environment of an electrochemical cell to chemically transform the structure and architecture of the membrane in a manner that enhances the transport selectivity of the membrane. The negative feedback loop associated with polysulfides reacting with PIM-7's phenazine subunits and then encountering restrictions in their access to deeper pore voids is both unusual and powerful in preventing the polysulfide shuttle. To that point, past work in ion-selective membranes would suggest that it is not possible to enhance the selective transport properties of the membrane without negatively impacting membrane conductivity. Our success in this regard highlights the power of directed evolution in defining new properties in ion-transporting membrane materials. In future schemes, we see the predictive design strategies, led by materials genomics as outlined here, as essential for tailoring the switching ability to any arbitrary battery chemistry. PIMs manifest as a universal platform to address crossover problems across a variety of battery architectures, whether solid-state and solution-based electrodes are employed. PIM membranes, adaptive and otherwise, therefore stand to significantly advance the field of electrochemical energy storage for aviation, transportation, and the grid.

ASSOCIATED CONTENT

Supporting Information

The Supporting Information is available free of charge on the ACS Publications website at DOI: 10.1021/acscentsci.7b00012.

Materials and methods, synthetic details, electrochemical methods, and other Supporting Information (PDF)

AUTHOR INFORMATION

Corresponding Author

*E-mail: bahelms@lbl.gov.

ORCID

Xiaohui Qu: 0000-0001-5651-8405

Brett A. Helms: 0000-0003-3925-4174

Notes

The authors declare no competing financial interest.

ACKNOWLEDGMENTS

A.L.W., X.Q., K.A.P., and B.A.H. were supported by the Joint Center for Energy Storage Research, an Energy Innovation Hub funded by the U.S. Department of Energy, Office of Science, Office of Basic Energy Sciences. S.E.D. was supported by the Department of Defense through the National Defense Science & Engineering Graduate Fellowship program. M.J.H. was supported in part by the U.S. Department of Energy, Office of Science, Office of Workforce Development for Teachers and Scientists (WDTS) under the Science Undergraduate Laboratory Internships Program (SULI). Portions of the work—including polymer synthesis and characterization, polymer processing, membrane testing, and Li−S battery testing—were carried out as a User Project at the Molecular Foundry, which is supported by the Office of Science, Office of Basic Energy Sciences, of the U.S. Department of Energy under Contract No. DE-AC02-05CH11231. The computational portion of this work used resources of the National Energy Research Scientific Computing Center, a DOE Office of Science User Facility supported by the Office of Science of the U.S. Department of Energy under the same contract. The Materials Project (BES DOE Grant No. EDCBEE) is acknowledged for infrastructure and algorithmic support. P. D. Frischmann is thanked for initial explorations of Li−S cell performance with PIM-1 and PIM-7 on Celgard.

REFERENCES

(1) Arora, P.; Zhang, Z. Battery Separators. *Chem. Rev.* **2004**, *104*, 4419−4462.

(2) Zhang, S. S. A review on the separators of liquid electrolyte Li-ion batteries. *J. Power Sources* **2007**, *164*, 351−364.

(3) Dunn, B.; Kamath, H.; Tarascon, J.-M. Electrical Energy Storage for the Grid: A Battery of Choices. *Science* **2011**, *334*, 928−935.

(4) Bruce, P. G.; Freunberger, S. A.; Hardwick, L. J.; Tarascon, J.-M. $Li-O_2$ and Li−S Batteries with High Energy Storage. *Nat. Mater.* **2012**, *11*, 19−29.

(5) Darling, R. M.; Gallagher, K. G.; Xie, W.; Su, L.; Brushett, F. R. Transport Property Requirements for Flow Battery Separators. *J. Electrochem. Soc.* **2016**, *163*, A5029−A5040.

(6) Mikhaylik, Y. V.; Akridge, J. R. Polysulfide shuttle study in the Li/S battery system. *J. Electrochem. Soc.* **2004**, *151*, A1969−A1976.

(7) Ji, X.; Lee, K. T.; Nazar, L. F. A Highly Ordered Nanostructured Carbon-Sulphur Cathode for Lithium−Sulphur Batteries. *Nat. Mater.* **2009**, *8*, 500−506.

(8) Yin, Y.-X.; Xin, S.; Guo, Y.-G.; Wan, L.-J. Lithium−Sulfur Batteries: Electrochemistry, Materials, and Prospects. *Angew. Chem., Int. Ed.* **2013**, *52*, 13186−13200.

(9) Yang, Y.; Zheng, G.; Cui, Y. Nanostructured Sulfur Cathodes. *Chem. Soc. Rev.* **2013**, *42*, 3018−3032.

(10) Busche, M. R.; Adelhelm, P.; Sommer, H.; Schneider, H.; Leitner, K.; Janek, J. Systematical electrochemical study on the parasitic shuttle-effect in lithium−sulfur cells at different temperatures and different rates. *J. Power Sources* **2014**, *259*, 289−299.

(11) Manthiram, A.; Fu, Y.; Chung, S.-H.; Zu, C.; Su, Y.-S. Rechargeable Lithium−Sulfur Batteries. *Chem. Rev.* **2014**, *114*, 11751−11787.

(12) Pang, Q.; Liang, X.; Kwok, C. Y.; Nazar, L. F. Review-The Importance of Chemical Interactions between Sulfur Host Materials and Lithium Polysulfides for Advanced Lithium−Sulfur Batteries. *J. Electrochem. Soc.* **2015**, *162*, A2567−A2576.

(13) Jin, Z.; Xie, K.; Hong, X.; Hu, Z.; Liu, X. Application of lithiated Nafion ionomer film as functional separator for lithium−sulfur cells. *J. Power Sources* **2012**, *218*, 163−167.

(14) Kim, M. S.; Ma, L.; Choudhury, S.; Archer, L. A. Multifunctional Separator Coatings for High-Performance Lithium−Sulfur Batteries. *Adv. Mater. Interfaces* **2016**, *3*, 1600450.

(15) Kim, M. S.; Ma, L.; Choudhury, S.; Moganty, S. S.; Wei, S.; Archer, L. A. Fabricating multifunctional nanoparticle membranes by a fast layer-by-layer Langmuir-Blodgett process: application in lithium−sulfur batteries. *J. Mater. Chem. A* **2016**, *4*, 14709−14719.

(16) Chung, S.-H.; Manthiram, A. Bifunctional Separator with a Light-Weight Carbon-Coating for Dynamically and Statically Stable Lithium−Sulfur Batteries. *Adv. Funct. Mater.* **2014**, *24*, 5299−5306.

(17) Budd, P. M.; Ghanem, B. S.; Makhseed, S.; McKeown, N. B.; Msayib, K. J.; Tattershall, C. E. Polymers of intrinsic microporosity (PIMs): robust, solution-processable, organic nanoporous materials. *Chem. Commun.* **2004**, 230−231.

DOI: 10.1021/acscentsci.7b00012
ACS Cent. Sci. 2017, 3, 399−406

(18) Budd, P. M.; Msayib, K. J.; Tattershall, C. E.; Ghanem, B. S.; Reynolds, K. J.; McKeown, N. B.; Fritsch, D. Gas separation membranes from polymers of intrinsic microporosity. *J. Membr. Sci.* **2005**, *251*, 263−269.
(19) McKeown, N. B.; Budd, P. M. Polymers of intrinsic microporosity (PIMs): organic materials for membrane separations, heterogeneous catalysis and hydrogen storage. *Chem. Soc. Rev.* **2006**, *35*, 675−683.
(20) Budd, P. M.; McKeown, N. B. Highly permeable polymers for gas separation membranes. *Polym. Chem.* **2010**, *1*, 63−68.
(21) McKeown, N. B.; Budd, P. M. Exploitation of Intrinsic Microporosity in Polymer-Based Materials. *Macromolecules* **2010**, *43*, 5163−5176.
(22) Longworth, R.; Vaughan, D. J. Physical structure of ionomers. *Nature* **1968**, *218*, 85−87.
(23) Kumar, S.; Pineri, M. Interpretation of small-angle x-ray and neutron scattering data for perfluorosulfonated ionomer membranes. *J. Polym. Sci., Part B: Polym. Phys.* **1986**, *24*, 1767−1782.
(24) Galambos, A. F.; Stockton, W. B.; Koberstein, J. T.; Sen, A.; Weiss, R. A.; Russell, T. P. Observation of cluster formation in an ionomer. *Macromolecules* **1987**, *20*, 3091−3094.
(25) Pannier, M.; Schädler, V.; Schöps, M.; Wiesner, U.; Jeschke, G.; Spiess, H. W. Determination of Ion Cluster Sizes and Cluster-to-Cluster Distances in Ionomers by Four-Pulse Double Electron Electron Resonance Spectroscopy. *Macromolecules* **2000**, *33*, 7812−7818.
(26) Qu, X.; Jain, A.; Rajput, N. N.; Cheng, L.; Zhang, Y.; Ong, S. P.; Brafman, M.; Maginn, E.; Curtiss, L. A.; Persson, K. A. The Electrolyte Genome Project: A Big Data Approach in Battery Materials Discovery. *Comput. Mater. Sci.* **2015**, *103*, 56−67.
(27) Cheng, L.; Assary, R. S.; Qu, X.; Jain, A.; Ong, S. P.; Rajput, N. N.; Persson, K.; Curtiss, L. A. Accelerating Electrolyte Discovery for Energy Storage with High-Throughput Screening. *J. Phys. Chem. Lett.* **2015**, *6*, 283−291.
(28) Jain, A.; Shin, Y.; Persson, K. A. Computational predictions of energy materials using density functional theory. *Nat. Rev. Mater.* **2016**, *1*, 15004.
(29) Aurbach, D.; Pollak, E.; Elazari, R.; Salitra, G.; Kelley, C. S.; Affinito, J. On the Surface Chemical Aspects of Very High Energy Density, Rechargeable Li−Sulfur Batteries. *J. Electrochem. Soc.* **2009**, *156*, A694−A702.
(30) Zhang, S. S. Role of $LiNO_3$ in rechargeable lithium/sulfur battery. *Electrochim. Acta* **2012**, *70*, 344−348.
(31) Rosenman, A.; Elazari, R.; Salitra, G.; Markevich, E.; Aurbach, D.; Garsuch, A. The Effect of Interactions and Reduction Products of $LiNO_3$, the Anti-Shuttle Agent, in Li−S Battery Systems. *J. Electrochem. Soc.* **2015**, *162*, A470−A473.
(32) Li, W.; Yao, H.; Yan, K.; Zheng, G.; Liang, Z.; Chiang, Y.-M.; Cui, Y. The synergetic effect of lithium polysulfide and lithium nitrate to prevent lithium dendrite growth. *Nat. Commun.* **2015**, *6*, 7436.
(33) Fang, W.; Zhang, L.; Jiang, J. Polymers of intrinsic microporosity for gas permeation: a molecular simulation study. *Mol. Simul.* **2010**, *36*, 992−1003.
(34) Heuchel, M.; Fritsch, D.; Budd, P. M.; McKeown, N. B.; Hofmann, D. Atomistic packing model and free volume distribution of a polymer with intrinsic microporosity (PIM-1). *J. Membr. Sci.* **2008**, *318*, 84−99.
(35) McDermott, A. G.; Budd, P. M.; McKeown, N. B.; Colina, C. M.; Runt, J. Physical aging of polymers of intrinsic microporosity: a SAXS/WAXS study. *J. Mater. Chem. A* **2014**, *2*, 11742−11752.
(36) Konnertz, N.; Ding, Y.; Harrison, W. J.; Budd, P. M.; Schönhals, A.; Böhning, M. Molecular Mobility of the High Performance Membrane Polymer PIM-1 as Investigated by Dielectric Spectroscopy. *ACS Macro Lett.* **2016**, *5*, 528−532.
(37) Staiger, C. L.; Pas, S. J.; Hill, A. J.; Cornelius, C. J. Gas Separation, Free Volume Distribution, and Physical Aging of a Highly Microporous Spirobisindane Polymer. *Chem. Mater.* **2008**, *20*, 2606−2608.
(38) Jue, M. L.; McKay, C. S.; McCool, B. A.; Finn, M. G.; Lively, R. P. Effect of Nonsolvent Treatments on the Microstructure of PIM-1. *Macromolecules* **2015**, *48*, 5780−5790.
(39) Gorgojo, P.; Karan, S.; Wong, H. C.; Jimenez-Solomon, M. F.; Cabral, J. T.; Livingston, A. G. Ultrathin Polymer Films with Intrinsic Microporosity: Anomalous Solvent Permeation and High Flux Membranes. *Adv. Funct. Mater.* **2014**, *24*, 4729−4737.
(40) Li, C.; Ward, A. L.; Doris, S. E.; Pascal, T. A.; Prendergast, D.; Helms, B. A. A Polysulfide-Blocking Microporous Polymer Membrane Tailored for Hybrid Li−Sulfur Flow Batteries. *Nano Lett.* **2015**, *15*, 5724−5729.
(41) Cuisinier, M.; Cabelguen, P.-E.; Evers, S.; He, G.; Kolbeck, M.; Garsuch, A.; Bolin, T.; Balasubramanian, M.; Nazar, L. F. Sulfur Speciation in Li−S Batteries Determined by Operando X-Ray Absorption Spectroscopy. *J. Phys. Chem. Lett.* **2013**, *4*, 3227−3232.
(42) Pascal, T. A.; Wujcik, K. H.; Velasco-Velez, J.; Wu, C.; Teran, A. A.; Kapilashrami, M.; Cabana, J.; Guo, J.; Salmeron, M.; Balsara, N.; Prendergast, D. X-Ray Absorption Spectra of Dissolved Polysulfides in Lithium−Sulfur Batteries from First-Principles. *J. Phys. Chem. Lett.* **2014**, *5*, 1547−1551.
(43) Wu, H.-L.; Huff, L. A.; Gewirth, A. A. In Situ Raman Spectroscopy of Sulfur Speciation in Lithium−Sulfur Batteries. *ACS Appl. Mater. Interfaces* **2015**, *7*, 1709−1719.
(44) Frischmann, P. D.; Gerber, L. C. H.; Doris, S. E.; Tsai, E. Y.; Fan, F. Y.; Qu, X.; Jain, A.; Persson, K. A.; Chiang, Y.-M.; Helms, B. A. Supramolecular Perylene Bisimide-Polysulfide Gel Networks as Nanostructured Redox Mediators in Dissolved Polysulfide Lithium−Sulfur Batteries. *Chem. Mater.* **2015**, *27*, 6765−6770.
(45) Fan, F. Y.; Carter, W. C.; Chiang, Y.-M. Mechanism and Kinetics of Li_2S Precipitation in Lithium−Sulfur Batteries. *Adv. Mater.* **2015**, *27*, 5203−5209.
(46) Gerber, L. C. H.; Frischmann, P. D.; Fan, F. Y.; Doris, S. E.; Qu, X.; Scheuermann, A. M.; Persson, K.; Chiang, Y.-M.; Helms, B. A. 3-Dimensional Growth of Li_2S in Lithium−Sulfur Batteries Promoted by a Redox Mediator. *Nano Lett.* **2016**, *16*, 549−554.
(47) Huang, J.-Q.; Zhang, Q.; Peng, H.; Liu, X.-Y.; Qian, W.-Z.; Wei, F. Ionic shield for polysulfides towards highly-stable lithium−sulfur batteries. *Energy Environ. Sci.* **2014**, *7*, 347−353.
(48) Bauer, I.; Thieme, S.; Bruckner, J.; Althues, H.; Kaskel, S. Reduced polysulfide shuttle in lithium−sulfur batteries using Nafion-based separators. *J. Power Sources* **2014**, *251*, 417−422.
(49) Zhang, Z.; Lai, Y.; Zhang, Z.; Zhang, K.; Li, J. Al_2O_3-coated porous separator for enhanced electrochemical performance of lithium sulfur batteries. *Electrochim. Acta* **2014**, *129*, 55−61.
(50) Li, W.; Hicks-Garner, J.; Wang, J.; Liu, J.; Gross, A. F.; Sherman, E.; Graetz, J.; Vajo, J. J.; Liu, P. V_2O_5 polysulfide anion barrier for long-lived Li−S batteries. *Chem. Mater.* **2014**, *26*, 3403−3410.
(51) Huang, J.-Q.; Zhuang, T.; Zhang, Q.; Peng, H.; Chen, C.; Wei, F. Permselective Graphene Oxide Membrane for Highly Stable and Anti-Self-Discharge Lithium−Sulfur Batteries. *ACS Nano* **2015**, *9*, 3002−3011.
(52) Bai, S.; Liu, X.; Zhu, K.; Wu, S.; Zhou, H. Metalorganic framework-based separator for lithium−sulfur batteries. *Nat. Energy* **2016**, *1*, 16094−16099.
(53) Hohenberg, P.; Kohn, W. Inhomogeneous Electron Gas. *Phys. Rev.* **1964**, *136*, B864−B871.
(54) Kohn, W.; Sham, L. J. Self-Consistent Equations Including Exchange and Correlation Effects. *Phys. Rev.* **1965**, *140*, A1133−A1138.
(55) Zhao, Y.; Truhlar, D. G. Exploring the Limit of Accuracy of the Global Hybrid Meta Density Functional for Main-Group Thermochemistry, Kinetics, and Noncovalent Interactions. *J. Chem. Theory Comput.* **2008**, *4*, 1849−1868.
(56) Tomasi, J.; Mennucci, B.; Cancés, E. The IEF version of the PCM solvation method: an overview of a new method addressed to study molecular solutes at the QM ab initio level. *J. Mol. Struct.: THEOCHEM* **1999**, *464*, 211−226.
(57) Shao, Y.; Gan, Z.; Epifanovsky, E.; Gilbert, A. T. B.; Wormit, M.; Kussmann, J.; Lange, A. W.; Behn, A.; Deng, J.; et al. Advances in

DOI: 10.1021/acscentsci.7b00012
ACS Cent. Sci. 2017, 3, 399−406

molecular quantum chemistry contained in the Q-Chem 4 program package. *Mol. Phys.* **2015**, *113*, 184−215.
(58) Ghanem, B. S.; McKeown, N. B.; Budd, P. M.; Fritsch, D. Polymers of Intrinsic Microporosity Derived from Bis(phenazyl) Monomers. *Macromolecules* **2008**, *41*, 1640−1646.
(59) Marenich, A. V.; Cramer, C. J.; Truhlar, D. G. Universal Solvation Model Based on Solute Electron Density and on a Continuum Model of the Solvent Defined by the Bulk Dielectric Constant and Atomic Surface Tensions. *J. Phys. Chem. B* **2009**, *113*, 6378−6396.
(60) Jeong, S.; Hu, L.; Lee, H. R.; Garnett, E.; Choi, J. W.; Cui, Y. Fast and Scalable Printing of Large Area Monolayer Nanoparticles for Nanotexturing Applications. *Nano Lett.* **2010**, *10*, 2989−2994.
(61) Rauh, R. D.; Abraham, K. M.; Pearson, G. F.; Surprenant, J. K.; Brummer, S. B. A lithium/dissolved sulfur battery with an organic electrolyte. *J. Electrochem. Soc.* **1979**, *126*, 523−527.
(62) Zu, C.; Fu, Y.; Manthiram, A. Highly reversible Li/dissolved polysulfide batteries with binder-free carbon nanofiber electrodes. *J. Mater. Chem. A* **2013**, *1*, 10362−10367.
(63) Fan, F. Y.; Woodford, W. H.; Li, Z.; Baram, N.; Smith, K. C.; Helal, A.; McKinley, G. H.; Carter, W. C.; Chiang, Y.-M. Polysulfide Flow Batteries Enabled by Percolating Nanoscale Conductor Networks. *Nano Lett.* **2014**, *14*, 2210−2218.
(64) Pope, M. A.; Aksay, I. A. Structural Design of Cathodes for Li−S Batteries. *Adv. Energy Mater.* **2015**, *5*, 1500124.
(65) Zhang, S.; Ueno, K.; Dokko, K.; Watanabe, M. Recent Advances in Electrolytes for Lithium−Sulfur Batteries. *Adv. Energy Mater.* **2015**, *5*, 1500117.
(66) Tikekar, M. D.; Choudhury, S.; Tu, Z.; Archer, L. A. Design principles for electrolytes and interfaces for stable lithium-metal batteries. *Nature Energy* **2016**, *1*, 16114.
(67) Lin, D.; Liu, Y.; Cui, Y. Reviving the lithium metal anode for high-energy batteries. *Nat. Nanotechnol.* **2017**, *12*, 194−206.

DOI: 10.1021/acscentsci.7b00012
ACS Cent. Sci. 2017, 3, 399−406